JOURNAL OF PHYSICAL ORGANIC CHEMISTRY
J. Phys. Org. Chem. 2003; **16:** 21–26
Published online in Wiley InterScience (www.interscience.wiley.com). DOI: 10.1002/poc.562

Cyclic hydrogen bond arrays: vibrational spectroscopic study of aminomethyl-substituted resorcinarene-based cavitands and their clathrates with THF

Jörg Dormann,[1]* Andreas Ruoff,[1] Jürgen Schatz,[2]* Oskar Middel,[3] Willem Verboom[3] and David N. Reinhoudt[3]

[1]Section of Vibrational Spectroscopy, University of Ulm, Albert-Einstein-Allee 11, D-89069 Ulm, Germany
[2]Division of Organic Chemistry I, University of Ulm, Albert-Einstein-Allee 11, D-89069 Ulm, Germany
[3]Laboratory of Supramolecular Chemistry and Technology, MESA$^+$ Research Institute, University of Twente, P.O. Box 217, NL-7500 AE Enschede, The Netherlands

Received 10 April 2002; revised 11 July 2002; accepted 15 July 2002

ABSTRACT: Mono- and tetrakis(aminomethyl)-substituted resorcinarene-based cavitands **1** and **2** and their clathrates $\mathbf{1}_2$·THF and **2**·$(THF)_2$ were investigated by FTIR spectroscopy and thermogravimetric analysis. Both hosts form stable clathrates with THF both in solution and in the solid state. Major intra- and intermolecular interactions could be identified and located by the use of vibrational spectroscopy. In all cases, dynamic cyclic intramolecular hydrogen bonds between the amino groups and neighbouring ether bridges are observable. Copyright © 2002 John Wiley & Sons, Ltd.

KEYWORDS: host–guest systems; resorcinarenes; calixarenes; supramolecular chemistry; vibrational spectroscopy

INTRODUCTION

The formation of hydrogen bonds is one of the major driving forces in supramolecular chemistry.[1,2] As a consequence, interest in the investigation of hydrogen-bonded systems is still growing. Fourier transform infrared (FTIR) spectroscopy is often used for this purpose, because this fast and efficient method can be applied to complexes in the gas, liquid and solid states. In the beginning of calixarene-related chemistry,[3–7] the cyclic hydrogen bond system at the lower rim fixing the cone conformation of these compounds was investigated by FTIR spectroscopy, proving the importance of this methodology.[3] Later, FTIR spectroscopy was used to characterize host–guest complexes of calixarenes[8–10] and resorcarene-based cavitands[11–13] in the solid state and in solution, especially with a focus on hydrogen-bonded[14–17] or surface-bound systems.[18,19]

Resorcinarene-based cavitands **1** and **2** (Scheme 1) seem to be predestined for inter- and intramolecular hydrogen bonds and also show a rich host–guest chemistry.[20] Therefore, we decided to use FTIR spectroscopy to study in cavitands **1** and **2** the weak supramolecular interactions which have a formative influence on the supramolecular, three-dimensional structure.

Correspondence to: J. Dormann, Section of Vibrational Spectroscopy, University of Ulm, Albert-Einstein-Allee 11, D-89069 Ulm, Germany.
E-mail: joerg.dormann@chemie.uni-ulm.de
Contract/grant sponsor: Deutsche Forschungsgemeinschaft; *Contract/grant number:* Scha 685/2-2; *Contract/grant number:* Scha 685/2-4.
Contract/grant sponsor: Fonds der Chemischen Industrie; *Contract/grant number:* Li 151/15.

RESULTS AND DISCUSSION

The syntheses of the resorcinarenes **1** and **2** have been described earlier.[21] When solid samples of the host molecules **1** and **2** were recrystallized from THF, stable clathrates with this solvent were formed. This is in agreement with solution studies on the complexation behaviour of both guest molecules and THF. By NMR titration experiments, an association constant of 500 $l\,mol^{-1}$ was found for THF as a guest and $CDCl_3$ as a solvent.[22] By thermogravimetric analysis,[23] a host-to-guest ratio of 2:1 for the monoamino cavitand **1** and 1:2 for host **2** could be deduced for the solid state. In the case of the complex $\mathbf{1}_2$·THF, the guest molecule leaves the crystal lattice at 320 K, whereas the first THF molecule of the **2**·$(THF)_2$ clathrate is liberated between 350 and 410 K and the second between 410 and 530 K. Therefore, the two THF molecules must sit on different sites in the crystal lattice, bound with different strengths in the crystal.

According to FTIR data, the cavitand **1** possesses low symmetry, the highest point group being C_s with one mirror plane through the NH_2 group, in case of deviation from this, C_1 is the corresponding point group. Host **2** is

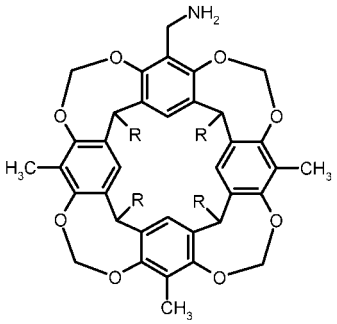

1 (R = C_5H_{11})

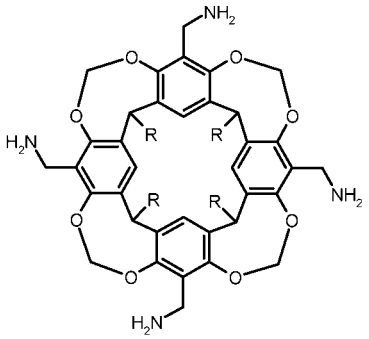

2 (R = C_5H_{11})

Scheme 1

of higher symmetry; the highest point group that can be assumed is C_{4v}, and if the methylamino groups are disordered the symmetry is lowered towards C_2 or C_1. The guest molecule (THF) exhibits C_{2v} symmetry in the case of a planar arrangement, otherwise a C_s or C_2 symmetry, and the site group is C_1. Therefore, for included THF, all modes are Raman and IR active, assuming C_s symmetry, the species are A and B whereas for C_1, the species is A.

Further details about the general procedure for the vibrational analysis of host–guest complexes can be found in the literature.[24,25]

In the $\mathbf{1}_2$·THF clathrate the THF guest molecule is bound strongly, as indicated by the thermogravimetric analysis; it can only be removed under severe conditions (heating, reduced pressure). This also applies to $\mathbf{2}$·$(THF)_2$.

FTIR spectroscopy reveals (Table 1) that most absorptions of the guest are shifted towards higher frequencies, the shift being up to $35\,cm^{-1}$ and the average shift about $16\,cm^{-1}$; some frequencies are shifted downwards, the shift being up to $57\,cm^{-1}$ and the average shift $22\,cm^{-1}$. This can be explained as a complexation-induced shift due to molecular interactions, which is very strong compared with similar shifts observed for the benzene and toluene complexes of the *p*-

Table 1. IR data for $\mathbf{1}_2$·THF

$\mathbf{1}_2$·THF				
293 K	80 K	Int.[a]	THF	Assignment[27,28]
—	3233 sh	*	3240	$\nu_{13} + \nu_{25} + \nu_{28}$
2955	2954	*	2966	ν_{18}
2861	2857	*	2826	ν_{21}
—	2336		2360	$2\nu_{10}$
1768	1768		1825	$2\nu_{13}$
1669	1669, 1645 sh	* 1, 2	1653	$\nu_7 + \nu_{17}$
1465 sh	1464 sh	*	1457	ν_6
1455 sh	1455 sh	*	1448	ν_{23}
1436 sh	1436 sh	*	—	$\nu_{15} + \nu_{32}$ B
1381	1385		1363	ν_7
1363	1363		1330	ν_8
1286	1292		1289	ν_{25}
1269	1272		1262	ν_{26}
1260	1259		1241	ν_9
1193	1194,	1, 2	1175	ν_{10}
1163	1168			
1071 sh	1079 sh, 1060 sh	* 1, 2	1069, 1060 sh	ν_{28}
1035 sh	1035 sh	*	1031	ν_{12}
883	927, 885		907	ν_{13}
816	817		803 sh	$\nu_{28} - \nu_{17}$ B
687 sh	684 sh, 662 sh	* 1, 2	656	ν_{16}
609 sh	609	*	601	ν_{32}

[a] Interpretation of band splittings; sh = shoulder; br = broad.
* Superposition of guest and host bands. 1, Different orientations of the host molecules in the crystal lattice. 2, Different orientations of the guest molecule in the host molecule or the crystal lattice.

Table 2. IR data for **2**·$(THF)_2$

2·$(THF)_2$				
293 K	80 K	Int.[a]	THF	Assignment[27,28]
3570 sh	3572		3568	$\nu_{18} + \nu_{32}$
3015, 2990	3017, 2994	1, 2	2993 sh	$\nu_{13} + \nu_{25} + \nu_{28}$
—	2980, 2968 sh	* 1, 2	2966	ν_{18}
2680 sh	2685		2680	$\nu_{23} + \nu_{26}$ A
1659 sh	1657		1653	$\nu_7 + \nu_{17}$
—	1459 sh	*	1457	ν_6
—	1454 sh	*	1448	ν_{23}
—	1439 sh	*	—	$\nu_{15} + \nu_{32}$ B
1343	sh, 1343	1, 2	1363	ν_7
1325 sh	1321		1330	ν_8
1284	1287, 1279	1, 2	1289	ν_{25}
1271	1268		1262	ν_{26}
—	1242 sh, 1232 sh	* 1, 2	1241	ν_9
1194 sh	1193, 1184 sh	* 1, 2	1175	ν_{10}
1068, 1056 sh	1072, 1067 sh, 1056 sh, 1046 sh	1, 2	1069, 1060 sh	ν_{28}
—	1039, 1032	1, 2	1031	ν_{12}
909	926, 909	1, 2	907	ν_{13}
662 sh	667 sh, 643	* 1, 2	656	ν_{16}
603	602		601	ν_{32}

[a] Interpretation of band splittings; sh = shoulder; br = broad.
* Superposition of guest and host bands. 1, Different orientations of the host molecules in the crystal lattice (one inside, one outside the cavity). 2, Different orientations of the guest molecule in the cavity.

tert-butylcalix[4,6]arenes. In the latter case, average shifts of 12–15 cm^{-1} can be found.[26]

Only a few absorption bands of THF are split into two components in the clathrate compared with the same absorptions in liquid THF. This could be caused by different orientations of the THF molecules in the crystal lattice or different interactions of one THF molecule with two differently orientated host molecules. The bandwidths observable for free THF in solution and enclathrated THF are similar. On the other hand, there are some bands which are typical of isolated molecules similar to the gas phase, e.g. ν_7 (Table 1). With respect to the thermogravimetric data and comparisons with other cavitates, interactions between enclathrated THF molecules are not likely. The similar behaviour is strictly related to the interactions, particularly to the hydrogen bonds. Another explanation is that the THF molecule is rotating inside the host.

Similarly to the FTIR spectra of cavitand **1**, most frequencies of THF are shifted towards higher frequencies when the solvent molecule is enclathrated by the host **2** forming a **2**·$(THF)_2$ complex (Table 2). The shift is up to 24 cm^{-1}, the average shift being about 9 cm^{-1}; some frequencies are shifted downwards, the shift being up to 20 cm^{-1} and the average shift 10 cm^{-1}.

In contrast to cavitand **1**, most bands of THF are split into two components upon clathrate formation. This is mostly caused by the different positions of the THF molecules with regard to the cavitand position and, derived from this, from different interactions of the THF molecules within the cavitand. Furthermore, different orientations of one THF molecule are also possible. Strikingly, one component of the splitting is strongly and the other one only moderately shifted. This indicates again that different interactions exist between the THF molecule inside the cavity and the other THF molecule placed outside. The bands of THF in solution and enclathrated THF are similar concerning the linewidth. However, interactions between a pair of THF molecules seem to be improbable.

A comparison of the FTIR spectra of free hosts (**1** and **2**) and guest (THF), respectively, and clathrates [**1**$_2$·THF or **2**·$(THF)_2$] shows that there are no significant shifts of the frequencies for the macrocyclic skeleton. This is in accordance with the rigid structure of the cavitands. However, when benzylamine is used as a model substance for the amino groups, the NH_2 absorptions are clearly changed (Tables 3–5).

The NH_2 bands are broadened by the NH—O hydrogen bonds. At room temperature there is only one band detectable, indicating a dynamic process in which these hydrogen bonds are involved. One possible explanation for this may be the rotation or switching of the NH_2 group as depicted in Scheme 2.

At low temperature (80 K), two NH_2 frequencies can be observed for cavitate **1**$_2$·THF, both absorptions being shifted towards lower frequencies (up to 60 cm^{-1}, Table 3). This gives evidence for further interactions with the NH_2 group, probably hydrogen bonding to the guest molecule.

In contrast, at room and low temperature, two NH_2 frequencies are observable for cavitand **2**. Both frequen-

Table 3. IR data for cavitand **1**, its clathrate $\mathbf{1}_2$·THF and benzylamine

		1[a]		$\mathbf{1}_2$·THF[a]	
	$PhCH_2NH_2$ 293 K	293 K	80 K	293 K	80 K
$\nu_{as}NH_2$	3378 s	3450 br	3374 (100%)[b]	3455 br	3368
ν_sNH_2	3296 s		3254		3236 (100%)[b]

[a] The relative intensities of $\nu_{as}NH_2$ and ν_sNH_2 are inverted; br = broad.
[b] Relative intensities.

Table 4. IR data for some shifted bands of cavitand **1** and its clathrate $\mathbf{1}_2$·THF

	1		$\mathbf{1}_2$·THF	
	293 K	80 K	293 K	80 K
Cavitand ring mode	625 588	624 589	623, 614 600, 586	623, 608 601, 588

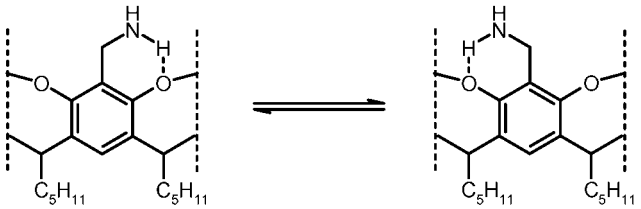

Scheme 2

cies are shifted towards lower frequencies (up to 58 cm^{-1}, Table 5); in the cavitate some frequencies are also shifted towards higher frequencies (up to 38 cm^{-1}, Table 5), but in most cases they are also shifted towards lower frequencies (up to 62 cm^{-1}, Table 5). The fact that the splitting of the NH_2 frequencies can be observed independently from included THF is evidence for different kinds of hydrogen bonds in which the NH_2 groups are involved. The intra-residue hydrogen bonding between the amino groups and the O-atom in the bridging units as described in Scheme 3 are very strong and thus strongly shifted towards lower frequencies. However, there is no driving force for the hydrogen bond networks to proceed around the rim in the same direction. In our opinion, we have to expect C_{2v} symmetry for the cavitand as shown in Scheme 3.

The maximum of the NH_2 frequencies is at about 3374 cm^{-1} in the case of cavitand **1**, whereas the maximum in the case of cavitand **2** is significantly lower (3239 cm^{-1}). This also indicates strong hydrogen bonds in the latter case. In contrast, we obtain two maxima with the same intensity for the ν_s NH_2 frequencies, when free cavitand **2** is compared with its THF complex. This can only be explained by a change within the hydrogen bonding network. The most probable explanation is that some of the amino groups also form hydrogen bonds towards the O-atom of the THF. This also means that the O-atom of the complexed THF is pointing out of the cavity. The second THF molecule is not interacting with the aminomethyl groups, otherwise further splittings should occur. This indicates that the second THF is situated outside the cavity and forms a clathrate.

Band splitting of some low-lying frequencies in two components, e.g. the cavitand ring mode at 588 cm^{-1} (cavitands **1** and **2**) and the ring mode at 850 cm^{-1} (cavitand **2**), can be explained as follows: in cavitand **1** it is an effect of the different orientation of the host units in the crystal lattice and the anisotropy of the potential field. This is not detectable in the case of a lower guest occupation. The intensities of the components are the same. This is in good agreement with the assumption of two differently orientated host molecules.

In cavitand **2**, the splitting is caused by the two THF molecules that are located at different places in the clathrate. The complexed THF molecule situated inside the cavity is in particular attached via hydrogen bonds; these are missing for the enclathrated THF molecule outside the cavity. In summary, the complexation-

Table 5. IR data for cavitand **2**, its clathrate **2**·$(THF)_2$ and benzylamine

		2[a]		**2**·$(THF)_2$[a]	
	$PhCH_2NH_2$ 293 K	293 K	80 K	293 K	80 K
$\nu_{as}NH_2$	3378 s	3409, 3371 (100%)[b]	3401, 3364	3415 (100%)[b] 3369	3391 sh 3363
ν_sNH_2	3296 s	3272 3193 3125 sh	3295 3239 (100%)[b] 3136 sh	3281 3205 —	3261 (100%)[b] 3234 (100%)[b] 3124 sh

[a] The relative intensities of $\nu_{as}(NH_2)$ and $\nu_s(NH_2)$ are inverted.
[b] Relative intensities.

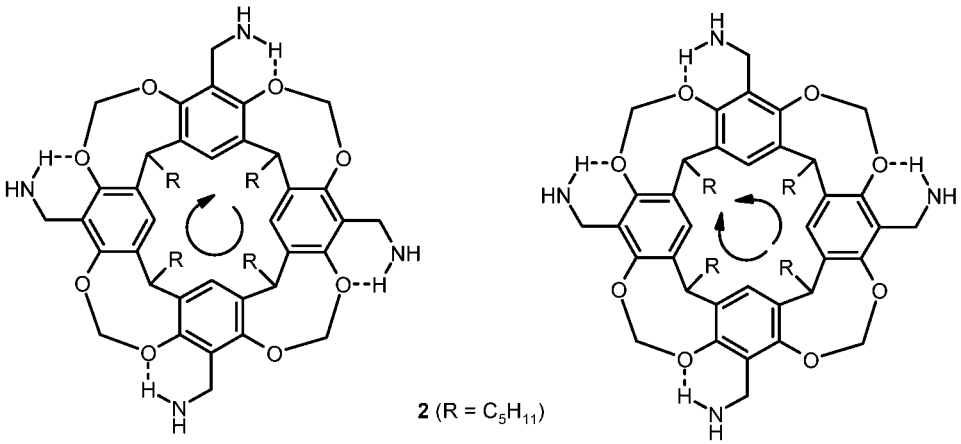

Scheme 3

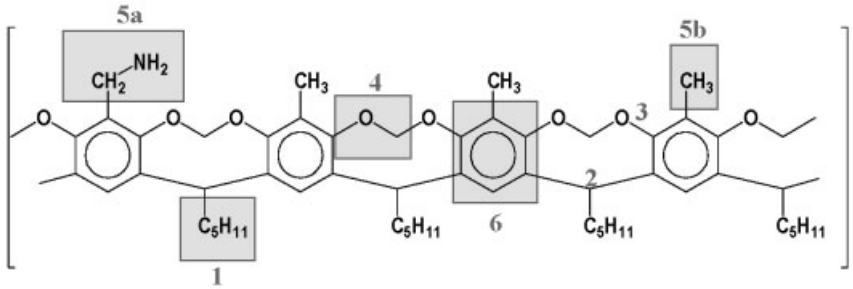

Scheme 4

induced shifts observed for the NH groups (cavitate $\mathbf{1}_2$·THF vs benzylamine as a model substance) indicate the following host–host and host–guest interactions (Scheme 4): CH–π interaction (part 1 and THF → part 6), hydrogen bonds (part 4 and THF → part 5a), induced dipole interaction (THF → part 4) and a further unspecified weak interaction (THF → part 1,5b).

Similar interactions can be specified for clathrate $\mathbf{2}\cdot(THF)_2$: CH–π interaction (part 1 → part 6, complexed/enclathrated THF → part 6), hydrogen bonds (part 4 and THF → part 5), induced dipole interaction (complexed THF → part 4) and a further unspecified weak interaction (enclathrated THF → part 1).

CONCLUSION

By the use of a thorough vibrational analysis of aminomethyl-substituted cavitands **1** and **2**, it is possible to describe the hydrogen bond array between the amino groups and the ether bridges fixing the macrocyclic skeleton. By the recently developed new strategy,[21] important host–guest interactions can be classified and good structural models based merely on FTIR data are accessible.

From the observed complex-induced shifts, three main types of interactions between host–host and host–guest can be located. Favourable CH–π and dipole interactions and mainly hydrogen bonds are responsible for the strong coherent structure of the clathrates.

EXPERIMENTAL

The syntheses of the cavitands **1** and **2** have been described earlier.[21] Infrared spectra (KBr pellets of pure crystalline samples) were recorded on an IFS 113v FTIR spectrophotometer (Bruker) using KBr windows and a DGTS detector, the resolution being about 0.5 cm^{-1}. The temperature of the samples was 293 and 80 K, respectively. Host-to-guest ratios of the samples used for the IR analysis were determined by thermogravimetric analysis as described earlier.[20]

Acknowledgements

This work was supported by the Deutsche Forschungsgemeinschaft (Scha 685/2-2 and 685/2-4) and the Fonds der Chemischen Industrie (Li 151/15). The generous

support Professor Dr G. Maas is gratefully acknowledged.

REFERENCES

1. Schneider H-J, Yatsimirsky A. *Principles and Methods in Supramolecular Chemistry*. Wiley: Chichester, 1999.
2. Steed JW, Atwood JL. *Supramolecular Chemistry*. Wiley-VCH: Weinheim, 2000.
3. Gutsche CD. Calixarenes. *Monographs in Supramolecular Chemistry*, Stoddart JF (ed), **vol. 1**. Royal Society of Chemistry: Cambridge, 1989.
4. Gutsche CD *et al*. Calixarenes: a Versatile Class of Macrocyclic Compounds. *Topics in Inclusion Science*, Vicens J, Böhmer V. (eds), **vol. 3**. Kluwer: Dordrecht, 1991.
5. Gutsche CD. *Calixarenes Revisited. Monographs in Supramolecular Chemistry*, Stoddart JF (ed), **vol. 6**. Royal Society of Chemistry: Cambridge, 1998.
6. Mandolini L, Ungaro R (eds). *Calixarenes in Action*. Imperial College Press: London, 2000.
7. Asfari Z, Böhmer V, Harrowfield J, Vicens J (eds). *Calixarenes 2001*. Kluwer: Dordrecht, 2001.
8. Schatz J, Schildbach F, Lentz A, Rastätter S, Schilling J, Dormann JM, Ruoff A, Debaerdemaeker T. *Z. Naturforsch., Teil B* 2000; **55**: 213–221.
9. Lutz BTG, Astarloa G, van der Maas JH, Janssen RG, Verboom W, Reinhoudt DN. *Vib. Spectrosc.* 1995; **10**: 29–40.
10. Paci B, Amoretti G, Arduini G, Ruani G, Shinkai S, Suzuki T. *Phys. Rev. B: Condens. Matter* 1997; **55**: 5566–5569.
11. Nissink JWM, Boerrigter H, Verboom W, Reinhoudt DN, van der Maas JH. *J. Chem. Soc., Perkin Trans. 2* 1998; 1671–1673.
12. Nissink JWM, Boerrigter H, Verboom W, Reinhoudt DN, van der Maas JH. *J. Chem. Soc., Perkin Trans. 2* 1998; 2541–2546.
13. Nissink JWM, Boerrigter H, Verboom W, Reinhoudt DN, van der Maas JH. *J. Chem. Soc., Perkin Trans. 2* 1998; 2623–2630.
14. Kanters JA, Schouten A, Steinwender E, van der Maas JH, Groenen LC, Reinhoudt DN. *J. Mol. Struct.* 1992; **269**: 49–64.
15. Brzezinski B, Urjasz H, Zundel G. *J. Phys. Chem.* 1996; **100**: 9021–9023.
16. Frkanec L, Visnjevac A, Kojic-Prodic B, Zinic M. *Chem. Eur. J.* 2000; **6**: 442–453.
17. Rudkevich DM. *Chem. Eur. J.* 2000; **6**: 2679–2682.
18. Moreira WC, Dutton PJ, Aroca R. *Langmuir* 1994; **10**: 4148–4152.
19. Nissink JWM, van der Maas JH. *Appl. Spectrosc.* 1999; **53**: 528–539.
20. Cram DJ. *Science* 1988; **240**: 760; Rudkevich DM, Rebek J Jr. *Eur. J. Org. Chem.* 1999; 1991–2005; Jasat AJ, Sherman JC. *Chem. Rev.* 1999; **99**: 931–967.
21. Boerrigter H, Verboom W, Reinhoudt DN. *J. Org. Chem.* 1997; **62**: 7148–7155; Boerrigter H, Verboom W, Reinhoudt DN. *Liebigs Ann. Rec.* 1997; 2247–2254.
22. Middel O, Verboom W, Reinhoudt DN. *J. Org. Chem.* 2001; **66**: 3998–4005.
23. Schatz J, Schildbach F, Lentz A, Rastätter S. *J. Chem. Soc., Perkin Trans. 2* 1998; 75–77.
24. Dormann JM, Ruoff A, Schatz J, Middel O, Verboom W, Reinhoudt DN. *J. Phys. Org. Chem.* 2001; **14**: 704–708.
25. Dormann JM, Ruoff A, Schatz J, Vysotsky M, Böhmer V. *J. Chem. Soc., Perkin Trans. 2* 2002; 83–87.
26. Dormann JM. Thesis, University of Ulm, 2002.
27. Cadioli M. *J. Phys. Chem.* 1993; **97**: 7848.
28. Varsányi G. *Assignments for Vibrational Spectra of Seven Hundred Benzene Derivatives*, vol. **1**. Adam Hilger: London, 1999.